



HAL
open science

Dynamic Covalent Chemistry Enables Reconfigurable All-Polysaccharide Nanogels

Fatma Abdi, Raphaël Michel, Robin Poirot, Malika Dakir, Lucie Sancey, Valérie Ravaine, Rachel Auzély-velty

► **To cite this version:**

Fatma Abdi, Raphaël Michel, Robin Poirot, Malika Dakir, Lucie Sancey, et al.. Dynamic Covalent Chemistry Enables Reconfigurable All-Polysaccharide Nanogels. *Macromolecular Rapid Communications*, 2020, 41 (15), pp.e2000213. <10.1002/marc.202000213>. <inserm-02941444>

HAL Id: inserm-02941444

<https://inserm.hal.science/inserm-02941444v1>

Submitted on 17 Sep 2020

HAL is a multi-disciplinary open access archive for the deposit and dissemination of scientific research documents, whether they are published or not. The documents may come from teaching and research institutions in France or abroad, or from public or private research centers.

L'archive ouverte pluridisciplinaire **HAL**, est destinée au dépôt et à la diffusion de documents scientifiques de niveau recherche, publiés ou non, émanant des établissements d'enseignement et de recherche français ou étrangers, des laboratoires publics ou privés.



HAL Authorization

Dynamic covalent chemistry enables reconfigurable all-polysaccharide nanogels

Fatma Abdi,^{‡a} Raphaël Michel,^{‡a} Robin Poirot,^a Malika Dakir,^b Lucie Sancey,^b Valérie Ravaine,^c Rachel Auzély-Velty^{*a}

^a Univ. Grenoble Alpes, Centre de Recherches sur les Macromolécules Végétales (CERMAV)-CNRS, 601, rue de la Chimie, BP 53, 38041 Grenoble Cedex 9 (France).

^b Univ. Grenoble Alpes, Institute for Advanced Biosciences, /INSERM U1209/ CNRS UMR5309, Grenoble, France.

^c Univ. Bordeaux, ISM, CNRS UMR 5255, Bordeaux INP, Site ENSCBP, 16 Avenue Pey Berland, 33607 Pessac Cedex, France.

ABSTRACT: Dynamic covalent bonds are established upon molecular recognition of sugar derivatives by boronic acid molecules. These reversible links can be used as crosslinking method to fabricate polymer-based responsive nanosystems. Herein, we report the design of the first dynamic nanogels entirely made of polysaccharides (PS). Based on PS chains alternately modified with phenyl boronic acid groups and sugar moieties, these colloids self-assemble in physiological conditions and combine the biocompatible nature of their PS backbone with the reconfiguration capacities of their crosslinking chemistry. These dynamic nanogels are easily prepared, long time stable, pH responsive and efficiently internalized by cancer cells.

Molecular recognition is a powerful tool to design soft nanoparticles used for diagnostics, chemical sensing and drug delivery.¹⁻³ In particular, the formation of boronic ester upon recognition of sugars by boronic acids attracts a growing attention as it results in dynamic covalent bonds that are stimuli-responsive.⁴ Accordingly, phenylboronic acid (PBA)-containing polymers have been used to design glucose-responsive nanosystems.⁴ For instance, responsive micelles have been prepared by self-assembly of PBA-containing block copolymers driven by hydrophobic interactions.⁵⁻⁷ Alternatively, some studies also demonstrated that the interaction between PBA and diol moieties can be used as driving force to form dynamic reconfigurable nanoparticles.⁸⁻¹¹ In this case, the dynamic covalent crosslinking grants the nanosystem with the ability to reorganize its molecular structure in response to the presence of a competing diol-containing molecule. Such nanosystem can thus be efficiently used for the controlled release of insulin triggered by the presence of glucose in the surrounding medium.¹² More recently, this approach was also applied to fabricate dynamic thermo- and pH-sensitive drug delivery vehicles for cancer treatment.¹³ Despite the potential of these boronic ester-crosslinked colloids for medical applications, the synthesis of such nanosystems consisting exclusively of PS has never been reported so far.

Polysaccharides are outstanding candidates for the design of such functional nanoparticles. Indeed, they are non-immunogenic, biocompatible, and biodegradable. Moreover, in spite of their functionalization by hydrophobic groups such as PBA, they remain water-soluble when they are charged, which prevents the use of organic cosolvent for nanoparticle formation contrarily to many synthetic polymers.¹³ Nevertheless, assembling such hydrophilic biopolymer building blocks, without any preconcentration technique, like water-in-oil emulsion,¹⁴⁻¹⁹ is highly challenging. It can be achieved using attractive partners,

typically oppositely charged macromolecules,^{14, 20-22} but the assembly of identical PS polyelectrolytes is hindered by electrostatic repulsion. Therefore, the nature of the molecular crosslinkers as well as the composition of the PS backbones are critical for the design of PS-based dynamic nanoassemblies.

Considering the unique biological properties of hyaluronic acid (HA) and its natural presence in tissues, we aimed at designing boronic ester crosslinked gel nanoparticles (also called nanogels) from this anionic PS. Previously, we successfully prepared dynamic covalent macrogels based on HA derivatives modified with a boronic acid moiety, and a maltose (or fructose) derivative.²³⁻²⁵ In physiological conditions, boronic ester crosslinks form between the two HA partners leading to a hydrogel with self-healing properties. In order to translate this approach to nanoscale materials, the balance between the associative property of the boronic ester cross-links and the electrostatic repulsion separating the anionic HA chains should be adjusted to promote nanoaggregate formation. Hence, our strategy is to replace one of the HA partners with Dextran (Dex), a neutral PS. Using HA modified with PBA (HA-PBA) and Dex functionalized with sugar moieties, we report the synthesis of original dynamic nanogels entirely made of biocompatible and biodegradable polysaccharides.

HA-PBA (Fig. 1A) is prepared by an amide coupling reaction between HA ($M_w = 100$ kg/mol) and 3-aminophenylboronic acid (the final degree of substitution (DS) is 0.18). Dex ($M_w =$

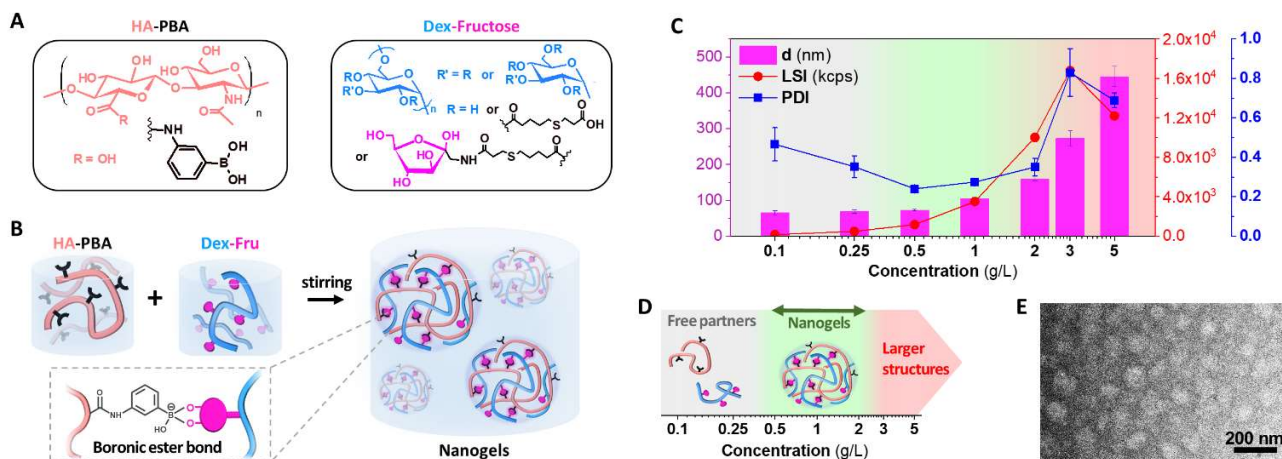


Figure 1. (A) Chemical structure of the PS partners HA-PBA and Dex-Fru. (B) Principle of nanogel formation upon creation of boronic ester crosslinks between PS partners. (C) DLS measurements of mixtures of PS partners at different concentrations displaying values of hydrodynamic diameter: d , scattering intensity: LSI, and the polydispersity index: PDI. (D) Schematic representation of the structure formed upon increasing the PS partner concentration. (E) Transmission electron microscopy image of nanogels at 1 g/L in PBS.

210 kg/mol) modified with fructose moieties (Fig. 1A) is obtained by an amide coupling reaction between 1-amino-1-deoxy-Fructosamine and Dex chains functionalized with mercaptopropionic acid molecules (DS = 0.2; synthetic routes are detailed in ESI).

From these PS partners in separate PBS solutions, nanoassemblies can be obtained by simply mixing both solutions (Fig. 1B) with a ratio between functional groups equal to one ($[PBA]/[Fru] = 1$). Nanogel formation is evidenced by dynamic light scattering (DLS, Fig. 1C) recording the hydrodynamic diameter (d) and polydispersity index (PDI) obtained by the method of cumulants.²⁶ Additionally, the light scattering intensity (LSI - expressed in counts per seconds) is followed as it represents the overall quantity of suspended scattering material and depends on particle size, concentration and refractive index.

From these DLS data, nanogel formation is found to occur only in a specific concentration range between 0.5 and 2 g/L. In fact, for concentration below 0.5 g/L, the values of the LSI (red dots on Fig. 1C) are very low and resemble those obtained with mixture of unmodified partners in the same conditions (see ESI – Fig. S13). This suggests that the partners are mostly present in the form of free chains in solution. This is further confirmed by the high PDI (blue squares in Fig. 1C) recorded for these low concentrated samples. For concentrations above 2 g/L, large polydisperse structures are present as evidenced by high values of d and PDI. Furthermore, the LSI decreases with increasing concentration showing that there are less scattering materials in the sample at 5 g/L than in the sample at 3 g/L. This indicates the sedimentation of some of the gel material which is confirmed by visual observation of a precipitate at the bottom of this more concentrated sample (Fig. S14). On the contrary, between 0.5 and 2 g/L, DLS results show the presence of relatively polydisperse ($PDI \leq 0.35$) nanoassemblies which size vary from 75 to 160 nm depending on the concentration. At 1 g/L, the nanogels formed have a typical size of 97 ± 5 nm and PDI equal to 0.25 ± 0.01 . TEM images corroborate this observation by showing nanostructures which smaller size (around 80 nm; see Fig. S17) can be explained by the drying of the sample on the TEM grid (Fig. 1E). Interestingly, for a given concentration, the nanoparticle size is not affected by the preparation method. Modifying the mixing mode and/or the order of introduction of

the partner solutions invariably leads to the same diameter (Fig. S12) confirming the robustness of this nanogel design. In the following, the nanogels formed at 1 g/L will be used for all further experiments.

The properties of the so-formed nanogels depend on the nature of the small molecular crosslinkers. This is demonstrated by comparing both fructose and maltose moieties grafted on Dex (see Fig. 1A and Fig. 2A). Firstly, just after preparation, the nanogels formed with maltose-functionalized dextran (Dex-Mal; DS = 0.22) in PBS have a slightly larger size than those formed with Dex-Fru (Fig. 2B). This is observed on all the tested samples (see Fig. S18), which suggests that this size difference is significant despite the relatively large PDI values recorded for these samples (≈ 0.25). Secondly, they also exhibit different long-term stability at room temperature. Although DLS measurements performed overtime (Fig. 2C) show a systematic size increase of both types of nanogels, the LSI of nanogels containing maltose decreases after about 30 hours of storage. This denotes a greater instability leading to sedimentation. On the contrary, nanogels containing fructose are stable for longer times as the first decrease in LSI is only observed after more than 170 hours (≈ 7 days) of storage. Both types of nanogels are metastable objects which temporary stability can be attributed to their net negative charges (ζ potential of -19 ± 1 mV in PBS for Dex-Fru/HA-PBA nanogels). The process of instability of these colloids is believed to occur through the fusion of nanogels until reaching a critical size forcing them to sediment. This is consistent with the progressive size increase observed in Fig. 2C and the observation of a precipitate after long storage time (Fig. S15). For these dynamic nanogels, fusion may be promoted by the dynamic exchange of boronic ester crosslinks between neighboring particles (see Fig. 2D). The subsequent bridging may bring the nanogels into contact and allow a structural rearrangement through exchange of boronic ester partners leading to larger objects. In this representation, the kinetics of instability relies on the exchange rate (k_{ex}) between partners: the quicker the exchange, the faster the process of fusion. Hence, the influence of the sugar moieties on the stability of nanogels could be explained by the difference in exchange rates between the partners: PBA/Fru and PBA/Mal. This hypothesis is in line with a recent work by us which demonstrates that the mechanical behavior of hydrogels crosslinked by

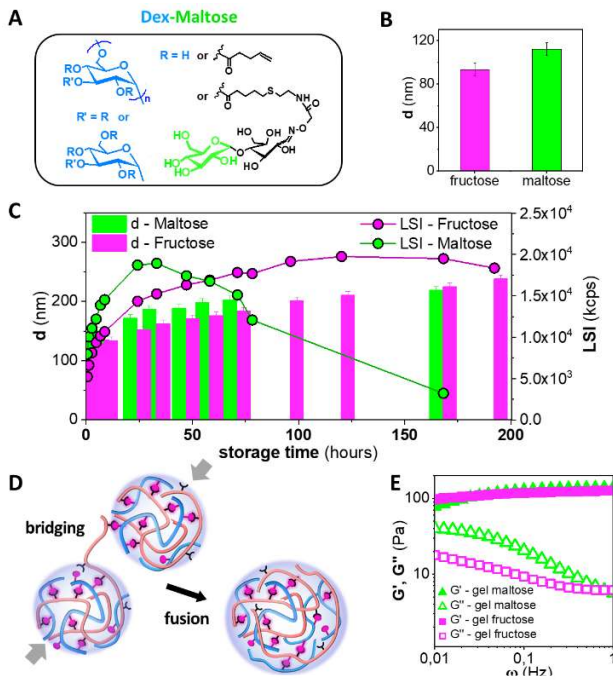


Figure 2: (A) Chemical structure of Dex-Mal. (B) Hydrodynamic diameter of nanogels formed with Dex-Fru and Dex-Mal just after preparation. (C) DLS measurements of fructose- and maltose-containing nanogels upon increasing storage time at RT. (D) schematic illustration of the bridging of neighboring nanogels and subsequent fusion. (E) Rheological measurements of fructose- and maltose-containing macrogels (15 g/L).

boronic ester bonds is essentially governed by the exchange kinetics of the boronic ester partners.²³ This confirms the key effect of k_{ex} on the dynamic properties of bulk materials.²⁷ Building on this knowledge and in order to confirm the key role of k_{ex} here, rheological measurements were performed on two macrogels (prepared at 15g/L in PBS) based on the PS partners, i.e. HA-PBA/Dex-Mal and HA-PBA/Dex-Fru. As shown in Fig. 2E, both materials exhibit a gel-like behavior ($G' > G''$) within the whole range of frequencies covered. The G' values in the plateau region of both assemblies are in the same order of magnitude (Fig. 2E). This indicates that the crosslinking densities, which are closely related to the binding constants of the PBA/saccharide complex,²³ are similar. However, the difference between the values of G' and G'' is much larger for the HA-PBA/Dex-Fru network than for the HA-PBA/Dex-Mal one. This suggests that the crossover frequency where $G' = G''$, which can be approximately considered as the inverse of the characteristic relaxation time of the network,²⁸ is lower for the HA-PBA/Dex-Fru mixture. In other words, the exchange rate of the PBA/Mal bond is faster since the dynamics of reversible networks is governed primarily by the network strand size and by the effective lifetime of reversible junctions.²⁹ As described above, this faster exchange may accelerate the process of fusion and explain the quicker instability observed for maltose-based nanogels (Fig. 2C). Since HA-PBA/Dex-Fru nanogels are more stable, they will be preferentially used in all further experiments.

Another interesting property of these nanogels is that after their formation at an appropriate concentration (1g/L), they can be diluted and remain stable (Fig. 3A) at a concentration for which they cannot be formed by mixing both partners (<0.5 g/L

– see Fig. 1C). Indeed, DLS measurements on diluted samples show that the concentration does not affect the diameter of the gel particles (Fig. 3B). Furthermore, the recorded LSIs for these diluted samples vary linearly with the concentration (Fig. 3C). This demonstrates that the nanogels are present in quantities proportional to their concentration thereby proving that no nanogels are disintegrating upon dilution. In comparison, intensities obtained with mixtures of unfunctionalized polysaccharides are much lower (Fig. 3C). In addition, these diluted samples age in a similar fashion to the more concentrated ones: they undergo a slow size increase over several days (Fig. S16).

While the nanogel structure is not influenced by dilution it is found to be greatly affected by pH conditions. This can be expected since boronic ester bond-cleavage is triggered by acidic conditions.³⁰ Accordingly, upon preparation in PBS at different

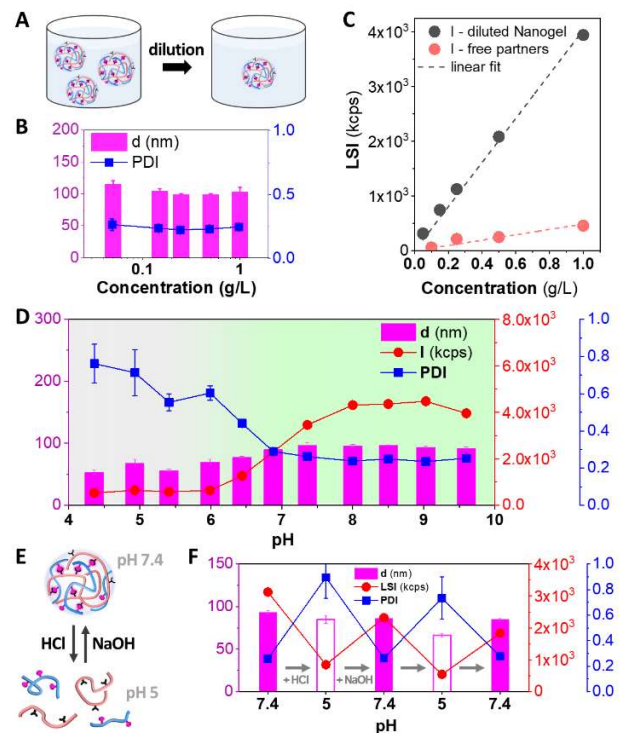


Figure 3: (A) Schematic illustration of the conservation of the nanogel integrity upon dilution. (B) DLS measurements of samples obtained by dilution of 1 g/L nanogel solutions. (C) LSI recorded on diluted nanogel samples (black circles) and samples containing unfunctionalized partners at the same concentrations (red circles). Linear fits are represented by dotted lines. (D) DLS measurements of samples at 1 g/L obtained by mixing the PS partners in PBS at different pH. (E) Schematic illustration of the pH responsiveness of nanogels. (F) DLS measurements of one nanogel sample (1g/L) submitted to a periodic change in pH (between 7.4 and 5).

pH, the DLS data show that nanogels are only formed for pH above 7 (Fig. 3D). For more acidic samples, the recorded LSIs are low and very similar to those obtained for the free partners in solution (see Fig. 3C - red circles). This shows that the PS partners are not associated at acidic pH. Interestingly, once formed at pH 7.4, the nanogels can be reversibly dismantled by lowering the pH as shown by the decrease of LSI and the increase of PDI upon adding HCl (Fig. 3F). Conversely, increasing again the pH of the same sample to 7.4 leads to an increase

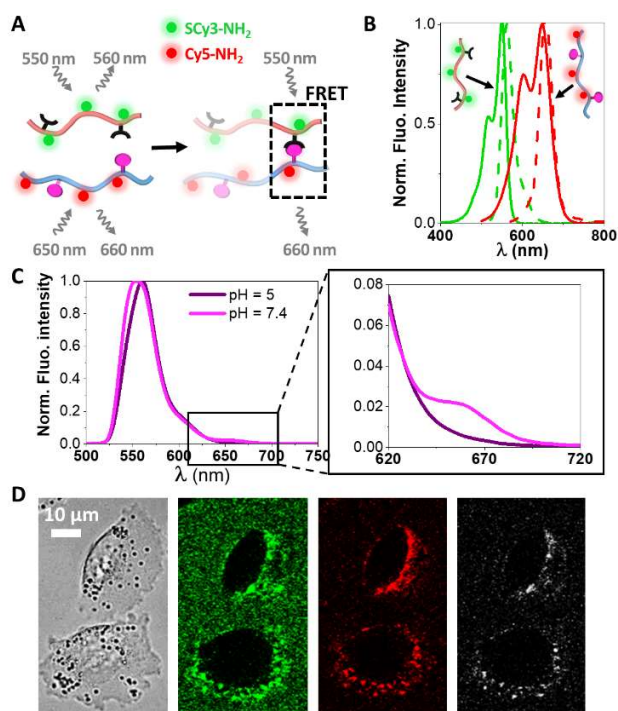


Figure 4: (A) schematic drawing of the labelled PS partners for FRET studies. (B) Intensity normalized absorption (solid line) and emission (dashed line) spectra of both labelled partners. (C) Normalized (at donor emission maxima) emission spectra ($\lambda_{ex} = 548$ nm) of mixtures of PS partners at different pH. (D) Confocal microscopy imaging of A375 melanoma cells after 30 min incubation with labelled nanogels displaying the signal emitted by SCy3 (green), Cy5 (red) and the FRET Signal (white).

in LSI and decrease in PDI (Fig. 3F) which suggest that nanogels are re-associating. This process of pH-driven dissociation/association can be repeated several times (Fig. 3F). The overall decrease in LSI seen on Fig. 3F can be attributed to the dilution of the system upon addition of NaOH and HCl.

In order to study the molecular structure of the nanogels as well as to probe their interaction with cells, Förster Resonance Energy Transfer (FRET)³¹ is used. More specifically, FRET allows to evaluate the molecular proximity of both PS partners thanks to a fluorescent donor-acceptor pair (Fig 4A).^{32, 33} To this aim, cyanine-based dyes SCy3-NH₂ (donor) and Cy5-NH₂ (acceptor)³⁴ are grafted with a relatively low degree of substitution on HA-PBA and Dex-Fru, respectively (DS = 0.02 and 0.01 respectively), so as not to alter the properties of the partners (see ESI for details on grafting method). The intensity normalized adsorption and emission spectra of the labelled polysaccharides are presented in Fig 4B. Upon mixing of both partners at pH 5, for which boronic ester bonds should not be formed, no FRET signal is observed (Fig. 4C – dark purple curve) confirming that both partners are free in the solution. On the contrary, at pH 7.4, a FRET peak is obtained at the characteristic wavelength (660 nm). This indicates that both partners are coming in close proximity through the formation of boronic ester crosslinks and confirm the molecular mechanism of its responsiveness to pH.

Finally, these nanogels have a great potential for biological application. This is the case firstly because their constitutive molecules (HA-PBA, Dex-Fru and Dex-Mal) are biocompatible. Indeed, they show no noticeable cytotoxicity on HEK293 kidney cells when introduced in concentrations similar to those

used for nanogel formation (Fig. S19). And secondly, because confocal images of labelled nanogels incubated for 30 minutes with cancer cells (A375 melanoma cells) show that nanogels are internalized within small vesicles in the cell cytoplasm (Fig. 4D). During their invagination, nanogels do not lose their integrity since the FRET signal is also visible on internalized objects (Fig. 4D - white signal on the right hand side). The first sign of nanogel dissociation, highlighted by a decrease in the FRET signal, was observed after more than 12 hours of incubation time.

In summary, dynamic nanogels exclusively made of PS can be obtained by simple mixing of negatively charged PS modified with PBA and neutral PS chains functionalized with sugar derivatives. The properties of the boronic ester crosslink responsible for the nanoassembly can be tuned by changing the sugar moieties or playing with the pH rendering these nanosystems highly versatile. Finally, these new nanogels are internalized by cancer cells thereby showing high potential for drug delivery purposes. Future work will focus on fine-tuning the stability and drug release of the nanogels by varying the degree of substitution of the PS and by integrating functional inorganic nanoparticles. Such versatile hybrid nanocolloids could offer an advanced platform for personalized therapy.

AUTHOR INFORMATION

Corresponding Author

* E-mail : rachel.auzely@cermav.cnrs.fr

Author Contributions

The manuscript was written through contributions of all authors. All authors have given approval to the final version of the manuscript.

‡These authors contributed equally.

Notes

The authors declare no conflict of interest.

ACKNOWLEDGMENT

Sanofi is acknowledged for funding Robin Poirot's PhD thesis. This work was also supported by the French funding agencies: FLI (France Life Imaging) for the project Thera-BODIPY, and the CNRS Mission for Transversal and Interdisciplinary Initiatives for the project BREVET-ISOTOP. The authors thank the NanoBio-ICMG Platform (FR 2607, Grenoble) for granting access to the Electron Microscopy facility.

REFERENCES

- Zhang, J.; Ma, P. X., Cyclodextrin-based supramolecular systems for drug delivery: Recent progress and future perspective. *Adv. Drug Delivery Rev.* **2013**, *65* (9), 1215-1233.
- de la Rosa, V. R.; Woisel, P.; Hoogenboom, R., Supramolecular control over thermoresponsive polymers. *Materials Today (Oxford, United Kingdom)* **2016**, *19* (1), 44-55.
- Li, D.; Qi, L., Self-assembly of inorganic nanoparticles mediated by host-guest interactions. *Curr. Opin. Colloid Interface Sci.* **2018**, *35*, 59-67.
- Ma, R.; Shi, L., Phenylboronic acid-based glucose-responsive polymeric nanoparticles: synthesis and applications in drug delivery. *Polym. Chem.* **2014**, *5* (5), 1503-1518.
- Liu, G.; Ma, R.; Ren, J.; Li, Z.; Zhang, H.; Zhang, Z.; An, Y.; Shi, L., A glucose-responsive complex polymeric micelle enabling repeated on-off release and insulin protection. *Soft Matter* **2013**, *9* (5), 1636-1644.

6. Wang, B.; Ma, R.; Liu, G.; Li, Y.; Liu, X.; An, Y.; Shi, L., Glucose-responsive micelles from self-assembly of poly(ethylene glycol)-b-poly(acrylic acid-co-acrylamidophenylboronic acid) and the controlled release of insulin. *Langmuir* **2009**, *25* (21), 12522-12528.
7. Zhao, L.; Ding, J.; Xiao, C.; He, P.; Tang, Z.; Pang, X.; Zhuang, X.; Chen, X., Glucose-sensitive polypeptide micelles for self-regulated insulin release at physiological pH. *J. Mater. Chem.* **2012**, *22* (24), 12319-12328.
8. Bapat, A. P.; Roy, D.; Ray, J. G.; Savin, D. A.; Sumerlin, B. S., Dynamic-Covalent Macromolecular Stars with Boronic Ester Linkages. *J. Am. Chem. Soc.* **2011**, *133* (49), 19832-19838.
9. Cheng, C.; Zhang, X.; Xiang, J.; Wang, Y.; Zheng, C.; Lu, Z.; Li, C., Development of novel self-assembled poly(3-acrylamidophenylboronic acid)/poly(2-lactobionamidoethyl methacrylate) hybrid nanoparticles for improving nasal adsorption of insulin. *Soft Matter* **2012**, *8* (3), 765-773.
10. Wang, Y.; Chai, Z.; Ma, L.; Shi, C.; Shen, T.; Song, J., Fabrication of boronic acid-functionalized nanoparticles via boronic acid-diol complexation for drug delivery. *RSC Adv.* **2014**, *4* (96), 53877-53884.
11. Wang, Y.; Zhang, X.; Mu, J.; Li, C., Synthesis and pH/sugar/salt-sensitivity study of boronate crosslinked glycopolymer nanoparticles. *New J. Chem.* **2013**, *37* (3), 796-803.
12. Ma, R.; Yang, H.; Li, Z.; Liu, G.; Sun, X.; Liu, X.; An, Y.; Shi, L., Phenylboronic Acid-Based Complex Micelles with Enhanced Glucose-Responsiveness at Physiological pH by Complexation with Glycopolymer. *Biomacromolecules* **2012**, *13* (10), 3409-3417.
13. Liu, H.-Y.; Qiao, Z.; Mao, X.-X.; Zha, J.-C.; Yin, J., Phenylboronic Acid-Dopamine Dynamic Covalent Bond Involved Dual-Responsive Polymeric Complex: Construction and Anticancer Investigation. *Langmuir* **2019**, *35* (36), 11850-11858.
14. Goycoolea, F. M.; Brunel, F.; Gueddari, N. E. E.; Coggiola, A.; Lollo, G.; Moerschbacher, B. M.; Remuñán-López, C.; Delair, T.; Domard, A.; Alonso, M. J., Physical Properties and Stability of Soft Gelled Chitosan-Based Nanoparticles. *Macromolecular Bioscience* **2016**, *16* (12), 1873-1882.
15. Lee, H.; Mok, H.; Lee, S.; Oh, Y.-K.; Park, T. G., Target-specific intracellular delivery of siRNA using degradable hyaluronic acid nanogels. *J Control Release* **2007**, *119* (2), 245-252.
16. Maiz-Fernández, S.; Pérez-Álvarez, L.; Ruiz-Rubio, L.; Pérez González, R.; Sáez-Martínez, V.; Ruiz Pérez, J.; Vilas-Vilela, L. J., Synthesis and Characterization of Covalently Crosslinked pH-Responsive Hyaluronic Acid Nanogels: Effect of Synthesis Parameters. *Polymers* **2019**, *11* (4).
17. Messenger, L.; Portecop, N.; Hachet, E.; Lapeyre, V.; Pignot-Paintrand, I.; Catargi, B.; Auzély-Velty, R.; Ravaine, V., Photochemical crosslinking of hyaluronic acid confined in nanoemulsions: towards nanogels with a controlled structure. *Journal of Materials Chemistry B* **2013**, *1* (27), 3369-3379.
18. Singh, S.; Möller, M.; Pich, A., Biohybrid nanogels. *Journal of Polymer Science Part A: Polymer Chemistry* **2013**, *51* (14), 3044-3057.
19. Solomko, N.; Budishevska, O.; Voronov, S.; Landfester, K.; Musyanovych, A., pH-Sensitive Chitosan-based Hydrogel Nanoparticles through Miniemulsion Polymerization Mediated by Peroxide Containing Macromonomer. *Macromolecular Bioscience* **2014**, *14* (8), 1076-1083.
20. Comert, F.; Malanowski, A. J.; Azarikia, F.; Dubin, P. L., Coacervation and precipitation in polysaccharide-protein systems. *Soft Matter* **2016**, *12* (18), 4154-4161.
21. Wu, D.; Delair, T., Stabilization of chitosan/hyaluronan colloidal polyelectrolyte complexes in physiological conditions. *Carbohydrate Polymers* **2015**, *119*, 149-158.
22. Zhang, Y.; Wang, F.; Li, M.; Yu, Z.; Qi, R.; Ding, J.; Zhang, Z.; Chen, X., Self-Stabilized Hyaluronate Nanogel for Intracellular Codelivery of Doxorubicin and Cisplatin to Osteosarcoma. *Advanced Science* **2018**, *5* (6), 1800811.
23. Figueiredo, T.; Cosenza, V.; Ogawa, Y.; Jeacomine, I.; Vallet, A.; Ortega, S.; Michel, R.; Olsson, J.; Gerfaud, T.; Boiteau, J.-G.; Jing, J.; Harris, C.; Auzély, R., Boronic acid and diol-containing polymers: how to choose the correct couple to form "strong" hydrogels at physiological pH. *Soft Matter* **2020**.
24. Figueiredo, T.; Jing, J.; Jeacomine, I.; Olsson, J.; Gerfaud, T.; Boiteau, J.-G.; Rome, C.; Harris, C.; Auzély-Velty, R., Injectable Self-Healing Hydrogels Based on Boronate Ester Formation between Hyaluronic Acid Partners Modified with Benzoxaborin Derivatives and Saccharides. *Biomacromolecules* **2020**, *21* (1), 230-239.
25. Tarus, D.; Hachet, E.; Messenger, L.; Catargi, B.; Ravaine, V.; Auzély-Velty, R., Readily Prepared Dynamic Hydrogels by Combining Phenyl Boronic Acid- and Maltose-Modified Anionic Polysaccharides at Neutral pH. *Macromol. Rapid Commun.* **2014**, *35* (24), 2089-2095.
26. Frisken, B. J., Revisiting the method of cumulants for the analysis of dynamic light-scattering data. *Appl. Opt.* **2001**, *40* (24), 4087-4091.
27. Cromwell, O. R.; Chung, J.; Guan, Z., Malleable and Self-Healing Covalent Polymer Networks through Tunable Dynamic Boronic Ester Bonds. *J. Am. Chem. Soc.* **2015**, *137* (20), 6492-6495.
28. Charlot, A.; Auzély-Velty, R., Novel Hyaluronic Acid Based Supramolecular Assemblies Stabilized by Multivalent Specific Interactions: Rheological Behavior in Aqueous Solution. *Macromolecules* **2007**, *40* (26), 9555-9563.
29. Leibler, L.; Rubinstein, M.; Colby, R. H., Dynamics of reversible networks. *Macromolecules* **1991**, *24* (16), 4701-4707.
30. Springsteen, G.; Wang, B., A detailed examination of boronic acid-diol complexation. *Tetrahedron* **2002**, *58* (26), 5291-5300.
31. Forster, T., Intermolecular energy transference and fluorescence. *Ann. Physik [6 Folge]* **1948**, *2*, 55-75.
32. Jares-Erijman, E. A.; Jovin, T. M., FRET imaging. *Nat. Biotechnol.* **2003**, *21* (11), 1387-1395.
33. Sapsford, K. E.; Berti, L.; Medintz, I. L., Materials for fluorescence resonance energy transfer analysis: beyond traditional donor-acceptor combinations. *Angew. Chem., Int. Ed.* **2006**, *45* (28), 4562-4588.
34. Roy, R.; Hohng, S.; Ha, T., A practical guide to single-molecule FRET. *Nat. Methods* **2008**, *5* (6), 507-516.

